The Effects of Stress Singularity on Welded Gusset Plates Loaded in Tension

J. KENT HSIAO, SUHENDI WIDJAJA, WILLIAM SCHULTZ, and STEVEN WIEMELER

Gusset plates in trusses or braced-frame structures (Figure 1) are generally used to transfer the applied forces from secondary elements (vertical and diagonal members in trusses or bracing members in braced frames) to main elements (top and bottom chords in trusses or beams and columns in braced frames) and vice versa. Therefore, the gusset plates should have sufficient strength and ductility to resist any tension, compression, and shear stress caused by the applied forces. Failure of the gusset plates can result in significant loss of strength throughout the entire structure.

The yielding, fracturing, bearing, and buckling failures due to tension, compression, and/or shear stresses are the main considerations for the design of steel gusset plates (Bjorhovde and Chakrabarti, 1985; Hardash and Bjorhovde, 1985; Bjorhovde, 1988; Astaneh-Asl, 1989; Gross, 1990; Astaneh-Asl, 1998; Cheng, Grondin, and Yam, 2000). When designing a gusset plate for a truss or a braced frame, structural engineers adjust the thickness, width, and/or length of the plate to mitigate the stresses that may cause fracturing of the gusset plate. The structural design profession, however, has traditionally neglected the stress concentration caused by the stress singularity (unbounded stress) effect due to the boundary condition at the corners of the fixed edges of the plate.

Stress singularities (unbounded stresses) may occur at the vertex of a sector plate with fixed-free radial edges as shown in Figure 2 if the plate is in tension and the vertex angle α lies between 63° and 180° (Williams, 1952). Note that for a structural steel plate with Poisson's ratio $\nu = 0.3$, stress singularities may occur if α lies between 61.3° (Hsiao, 2000) and 180°. Consider a steel gusset plate that is subjected to tension as shown in Figure 3; the angle α_1 at the right-hand fixed-free corner is 90° while the angle α_2 at the left-hand fixed-free corner is larger than 90°. Since both the α_1 and α_2 angles lie between 61.3° and 180°, stress concentration may occur at these corners due to the stress singularity effect.

The configurations of the corners with fixed-free radial edges of the gusset plate shown in Figure 3 are similar to that of the gusset plates of the test specimen AW18 (a double-

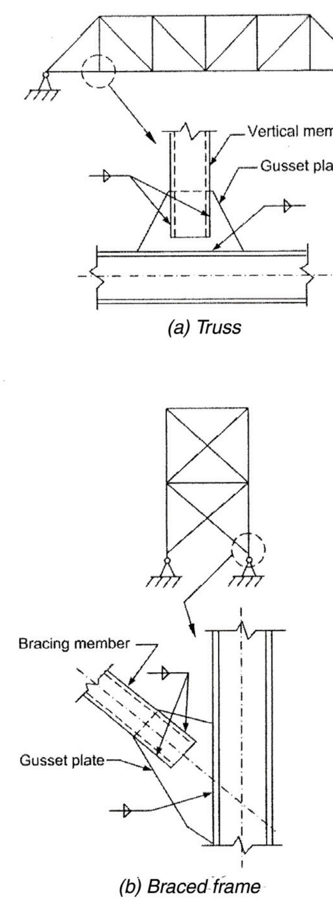

Fig. 1. Truss and braced frame with gusset plate connections.

J. Kent Hsiao is assistant professor, department of civil and environmental engineering, Southern Illinois University, Carbondale, IL.

Suhendi Widjaja is a graduate student, department of civil and environmental engineering, Southern Illinois University, Carbondale, IL.

William Schultz is a graduate student, department of civil and environmental engineering, Southern Illinois University, Carbondale, IL.

Steven Wiemeler is a graduate student, department of civil and environmental engineering, Southern Illinois University, Carbondale, IL.

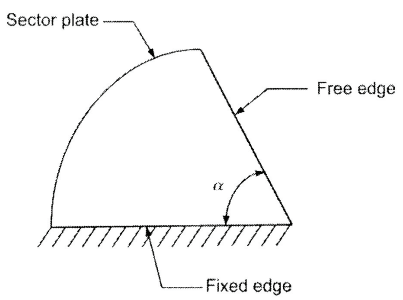

Fig. 2. Sector plate with fixed-free radial edges.

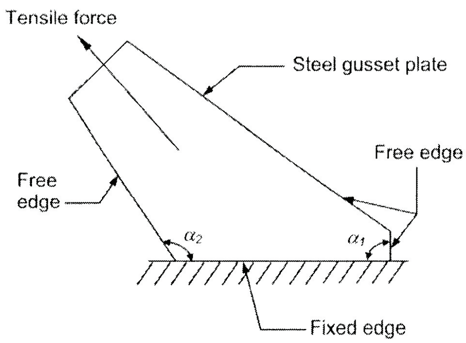

Fig. 3. Steel gusset plate with fixed-free radial edges.

angle brace with end gusset plates) conducted by Astaneh-Asl, Goel, and Hanson (1982). According to their test for the cyclic behavior of the welded brace member-gusset plate assembly specimen, a crack in the gusset plate occurred (Figure 4) during the last cyclic tension deformation of the specimen. The crack was caused by the stress concentration at the corner. Since the angle of the cracked corner lies between 61.3° and 180°, a stress concentration occurred at the corner due to the stress singularity effect when the plate was under tension.

Based on the bracing member size and the gusset plate configuration of the specimen AW18 tested by Astaneh-Asl and others (1982), a finite element model for the welded brace member-gusset plate assembly was created (Figure 5)

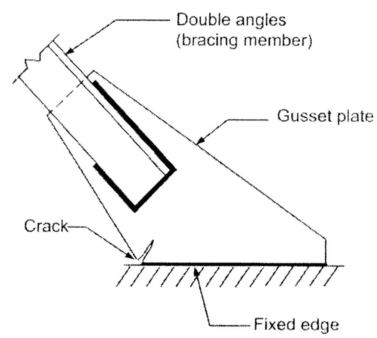

Fig. 4. Crack in gusset plate .

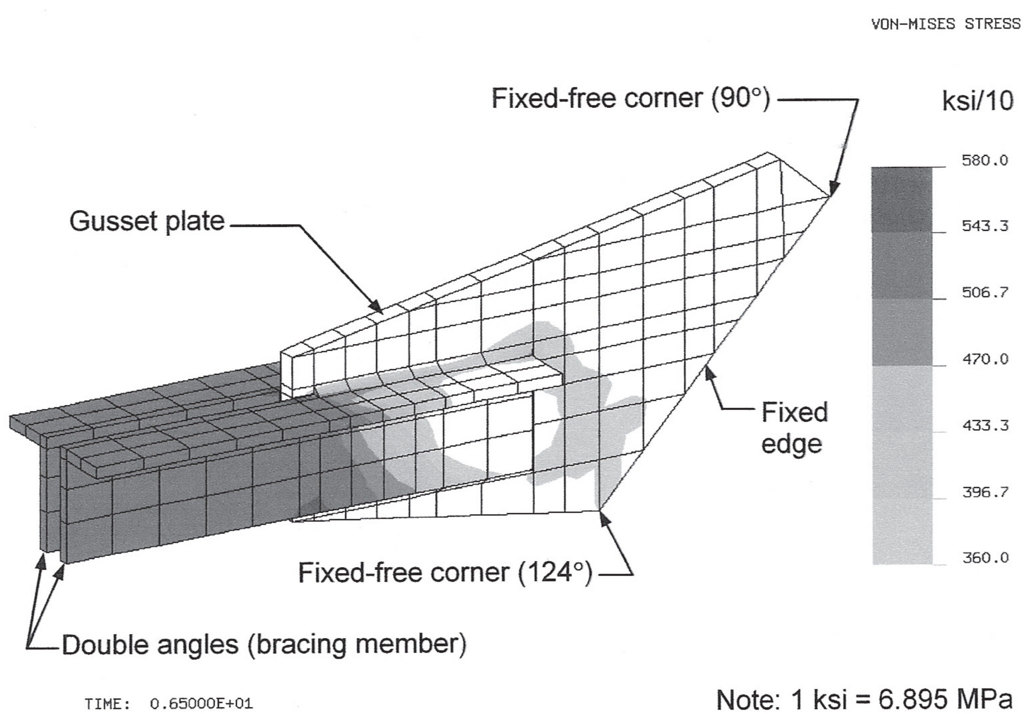

Fig. 5. Von Mises stress distribution on gusset plate due to the stress singularity effect.

in order to investigate the effects of stress singularity on the gusset plate. Nonlinear static analysis was conducted for the model using the computer software NISA/DISPLAY (NISA, 1998). The result of the tension analysis for the assembly is shown in Figure 5. Note that ASTM A36 steel was used for both the gusset plate and the bracing member. The elastic, piecewise linear hardening stress-strain curve shown in Figure 6 [derived from Salmon and Johnson (1996)] for A36 steel was used for the analysis. Also note that the E7018 electrode was used for the fillet weld. The elastic, linear hardening stress-strain curve shown in Figure 7 [derived from the Lincoln Electric Company (1994)] was used as the material property of the E7018 electrode for the fillet weld.

The double angles used for the model shown in Figure 5 are 2L-2½ × 1½ × ¼. The angles were welded to both sides of a ½-in.-thick (13 mm) gusset plate. In order to consider the effect of strain hardening of the steel as shown in Figure 6, an arbitrary tensile stress of 80 ksi (550 MPa) was applied at the free end of the double angles. A pseudo time of 10.0 was used for the time span that is equivalent to load increments or steps [from zero to 80 ksi (550 MPa)]. When the time step reached 6.5 as shown in Figure 5, the applied stress at the free end of the double angle reached 52 ksi (360 MPa) [= 80 ksi × (6.5/10)]. At this time step, the von Mises stress (related to yielding) exceeded 36 ksi (250 MPa) at the 124° fixed-free corner. Note that only the stresses that are larger than 36 ksi (250 MPa) are shown in the figure. Also note that since both the 124° fixed-free corner and the 90° fixed-free corner lie between 61.3° and 180°, the stress concentration started at the larger fixed-free corner (in other words, the 124° fixed-free corner) as shown in Figure 5. The development of the stress concentration at the vertex of the corner was then expedited due to the stress singularity effect and therefore resulted in yielding and fracturing at the corner as shown in Figure 4.

The investigation using the finite element method conducted above demonstrated that the configuration (the degree of angle) of the fixed-free corner plays a very important role in the design strength and the ductility capacity of the steel gusset plate when the plate is subjected to tensile forces.

INTERACTION BETWEEN STRESS SINGULARITY EFFECT AND WHITMORE EFFECTIVE WIDTH

The effective width of the Whitmore section for a welded joint can be defined as the distance l_w as shown in Figure 8 (Whitmore, 1952; AISC, 2001). The line that passes through the end of the welded joint end is intersected at points P_1 and P_2 by the two lines spreading the force from the start of the welded joint 30° to each side of the welded joint. The distance l_w is measured from point P_1 to P_2 along the line that passes through the end of the welded joint.

It is interesting to note that there is a relationship between the critical angle for the Whitmore effective width and the critical angle for the stress singularity effect. Referring to Figure 8, the relationship between these two angles is 61.3° (the critical angle for the stress singularity effect) ≈ 90° – 30° (the critical angle for the Whitmore effective width). In order to investigate the interaction between the stress singularity effect and the location of the Whitmore lines, numerous

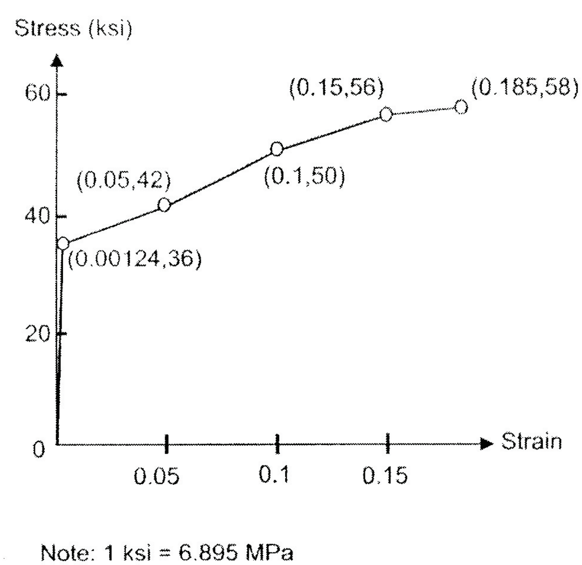

Fig. 6. Elastic, piecewise linear hardening stress-strain curve for ASTM A36 steel.

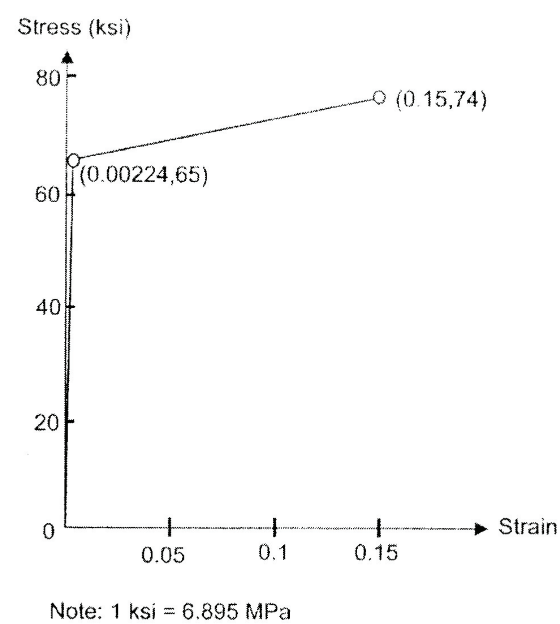

Fig. 7. Elastic, linear hardening stress-strain curve for E7018 electrode.

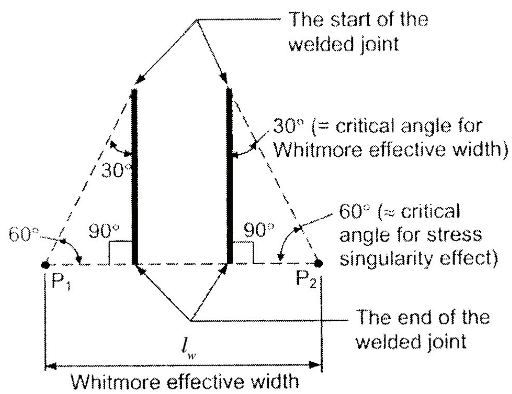

Fig. 8. Whitmore effective width for a welded joint.

finite element models with various locations of Whitmore lines have been constructed and analyzed. The results of the finite element analysis of the following six models (A1, A2, A3, B1, B2, and C1 as shown in Figures 9, 10, 11, 12, 13, and 14) represent the results of the investigation.

Gusset Plate Models A1, A2, and A3

Models A1, A2, and A3 have been constructed to simulate the possible configurations of a gusset plate for a 90° bracing-member-to-main-member connection.

Figure 9 presents the gusset plate model A1. Figure 9(a) illustrates that the angle at each of the fixed-free corners of the plate is about 67°. Also, the 30° Whitmore lines begin from the start of the welded joint and end at the fixed-free corners. As shown in Figure 9(a), the total area of the critical

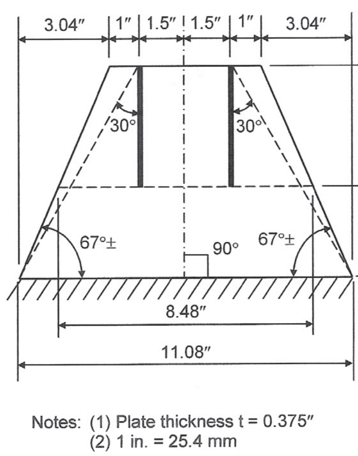

(a) Dimensions of gusset plate

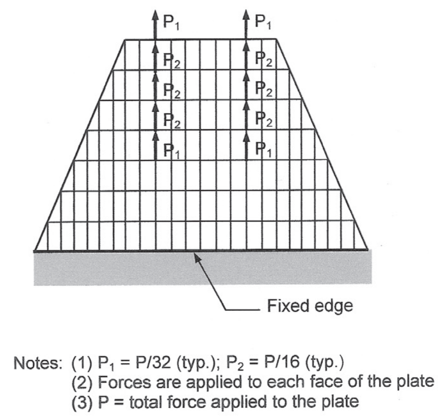

(b) Computer model and applied forces

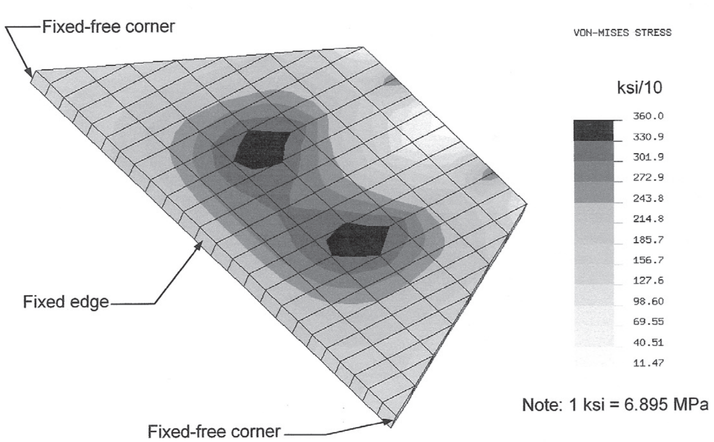

(c) Von Mises stress distribution at P = 88.1 kips (392 KN)

Fig. 9. Gusset plate model A1 for a 90° bracing-member-to-main-member connection.

cross section along the line that passes through the end of the welded joint is 3.18 in.^{2} (2050 mm^2) (= 8.48 in. × 0.375 in.). The computer model of the gusset plate, as well as the forces that are applied to the plate, are shown in Figure 9(b). Yielding starts at the end of the welded joint [where the von Mises stress reaches 36 ksi (250 MPa)] when the total applied tensile force, *P*, reaches 88.1 kips (392 kN) as shown in Figure 9(c).

Figure 10 presents the gusset plate model A2. Figure 10(a) illustrates that the angle at each of the fixed-free corners of the plate is about 75°. Also, the 30° Whitmore lines begin from the middle of the welded joint and end at the fixed-free corners. As shown in Figure 10(a), the total area of the critical cross section along the line that passes through the end of the welded joint is 3.15 in.^{2} (2030 mm^2) (= 7.16 in. × 0.44 in.). The computer model of the gusset plate, as well as the forces that are applied to the plate, are shown in Figure 10(b). Yielding starts at the end of the welded joint when the total applied tensile force, *P*, reaches 101.9 kips (453 kN) as shown in Figure 10(c).

Figure 11 presents the gusset plate model A3. Figure 11(a) illustrates that the angle at each of the fixed-free corners of the plate is 90°; also, the 30° Whitmore lines (beginning either from the start or the middle of the welded joint) end outside the areas of the fixed-free corners. As shown in Figure 11(a), the total area of the critical cross section along the line that passes through the end of the welded joint is 3.15 in.^{2} (2030 mm^2) (= 5 in. × 0.63 in.). The computer model of the gusset plate, as well as the forces that are applied to the plate, are shown in Figure 11(b). Yielding starts at the fixed-free corners when the total applied tensile force, *P*, reaches 84.0 kips (374 kN) as shown in Figure 11(c).

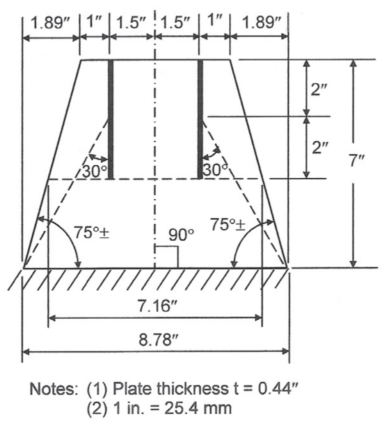

(a) Dimensions of gusset plate

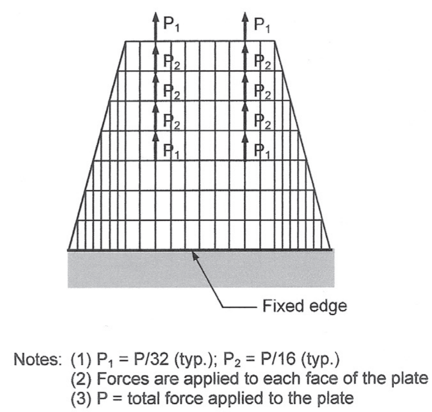

(b) Computer model and applied forces

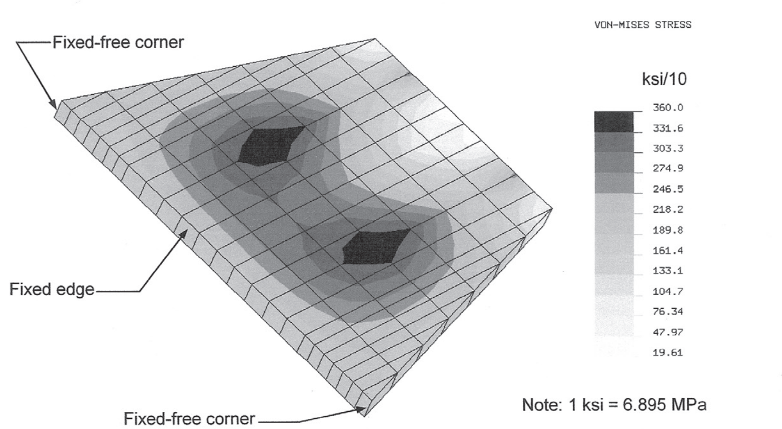

(c) Von Mises stress distribution at P = 101.9 kips (453 KN)

Fig. 10. Gusset plate model A2 for a 90° bracing-member-to-main-member connection.

The following conclusions are drawn from the results of the finite element analysis of plates A1, A2, and A3:

1. Both plates A1 and A2 start yielding at their critical cross-sections. Although the total area of the critical cross-section of plate A1 is slightly larger than that of plate A2 [3.18 in.^{2} (2050 mm^2) versus 3.15 in.^{2} (2030 mm^2)], plate A1 exhibits a smaller tensile yielding capacity than that of plate A2 [88.1 kips (392 kN) versus 101.9 kips (453 kN)]. Note that the yielding capacity and the thickness of the plate are directly related by a ratio [88.1 kips/101.9 kips) ≈ (0.375 in./0.44 in.)]. Therefore, if yielding is expected to start at the critical cross-section (in other words, at the end of the welded joint) of a gusset plate, the tensile yielding capacity of the gusset plate can be increased more effectively by increasing the thickness of the plate rather than the width of the plate.

2. Plate A3 starts yielding at its fixed-free corners. Although the total area of the critical cross-section of plate A3 [3.15 in.^{2} (2030 mm^2)] is almost the same as that of plates A1 and A2, plate A3 exhibits the smallest tensile yielding capacity 84.0 kips (374 kN) due to the stress singularity effect on the fixed-free corners. Therefore, if yielding is expected to start at the fixed-free corners of a gusset plate, the tensile yielding capacity of the gusset plate can be increased more effectively by increasing the width at the base of the plate rather than the thickness of the plate. Increasing the width at the base of the plate will reduce the angle at the fixed-free corners, which in turn will mitigate the stress singularity effect at these corners.

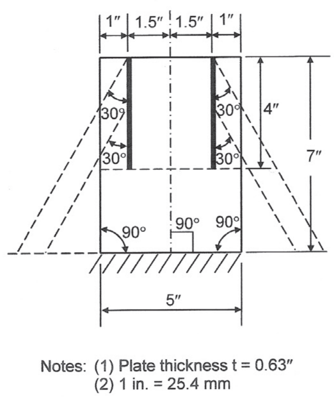

(a) Dimensions of gusset plate

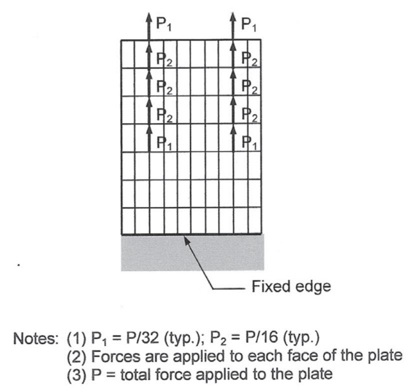

(b) Computer model and applied forces

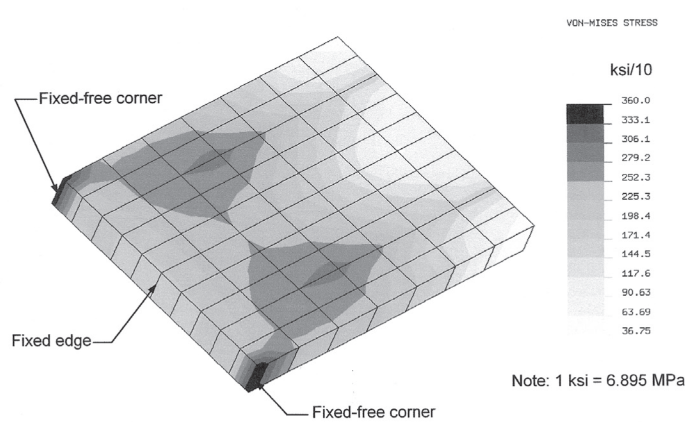

(c) Von Mises stress distribution at P = 84.0 kips (374 KN)

Fig. 11. Gusset plate model A3 for a 90° bracing-member-to-main-member connection.

Gusset Plate Models B1 and B2

Models B1 and B2 have been constructed to simulate the possible configurations of a gusset plate for a 45° bracing-member-to-main-member connection.

Figure 12 presents the gusset plate model B1. Figure 12(a) illustrates that the angle at each of the fixed-free corners of the plate is 114° (at the right side) and 60° (at the left side), respectively. Also, the right-side Whitmore line begins from the start of the welded joint and ends at the 114° fixed-free corner. The left-side Whitmore line begins from the end of the welded joint and ends at the top of the free edge with a 60° fixed-free corner. As shown in Figure 12(a), the total area of the critical cross section along the line that passes through the end of the welded joint is 3.8 in.^{2} (2450 mm^2) (= 7.6 in. × 0.5 in.). The computer model of the gusset plate, as well as the forces that are applied to the plate, are shown in Figure 12(b). Yielding starts at the 114° fixed-free corner [where the von Mises stress reaches 36 ksi (248 MPa)] when the total applied tensile force, P, reaches 100.8 kips (448 kN) as shown in Figure 12(c).

Figure 13 presents the gusset plate model B2. Figure 13(a) illustrates that the angle at each of the fixed-free corners of the plate is 126° (at the right side) and 60° (at the left side), respectively. Also, the right-side Whitmore line begins from the middle of the welded joint and ends at the 126° fixed-free corner. The left-side Whitmore line begins from the end of the welded joint and ends at the top of the free edge with a 60° fixed-free corner. As shown in Figure 13(a), the total area of the critical cross section along the line that passes through the end of the welded joint is 3.78 in.^{2} (2440 mm^2) (= 6.4 in. × 0.59 in.). The computer model of the gusset plate, as well

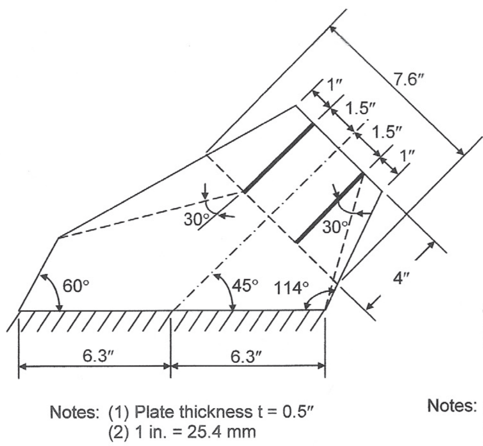

(a) Dimensions of gusset plate

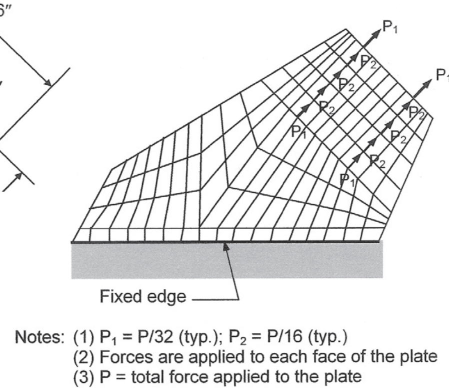

(b) Computer model and applied forces

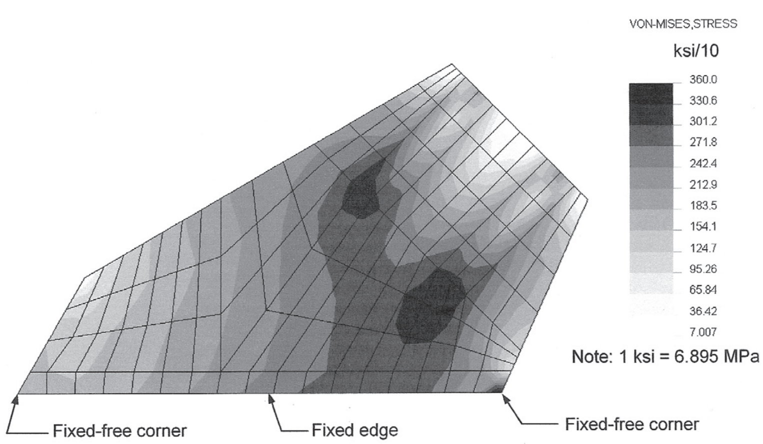

(c) Von Mises stress distribution at P = 100.8 kips (448 KN)

Fig. 12. Gusset plate model B1 for a 45° bracing-member-to- main-member connection.

as the forces that are applied to the plate, are shown in Figure 13(b). Yielding starts at the 126° fixed-free corner when the total applied tensile force, *P*, reaches 85.3 kips (379 kN) as shown in Figure 13(c).

The following conclusions are drawn from the results of the finite element analysis of plate B1 and B2:

Both plates B1 and B2 start yielding at the fixed-free corner with an obtuse angle (in other words, the 114° angle of plate B1 and the 126° angle of plate B2). Although the total area of the critical cross section of plate B2 is almost the same as that of plate B1 [3.78 in.^{2} (2440 mm^2) versus 3.8 in.^{2} (2450 mm^2)], plate B2 exhibits a much smaller tensile yielding capacity than that of plate B1 [85.3 kips (379 kN) versus 100.8 kips (448 kN)] due to the significant stress singularity effect on the 126° fixed-free corner of plate B2. Therefore, the tensile yielding capacity of the gusset plate B2 can be increased more effectively by increasing the length at the base of the plate rather than the thickness of the plate (for example, plate B1 versus plate B2). Increasing the length at the base of the plate will reduce the obtuse angle at the fixed-free corner, which in turn will mitigate the stress singularity effect at the corner.

Gusset Plate Model C1

The model C1 has been constructed to simulate the possible configurations of a gusset plate for a 67.5° bracing- member-to-main-member connection.

Figure 14 presents the gusset plate model C1. Figure 14(a) illustrates that the angle at each of the fixed-free corners of the plate is 98° (at the right side) and 53° (at the left side), respectively. Also, the right-side Whitmore line begins at a distance of 1 in. (25 mm) from the start of the welded joint and ends at the 98° fixed-free corners. The left-side Whitmore line begins at a distance of 3 in. (76 mm) from the start of the welded joint and ends at the 53° fixed-free corner. The computer model of the gusset plate, as well as the forces that are applied to the plate, are shown in Figure 14(b). Yielding

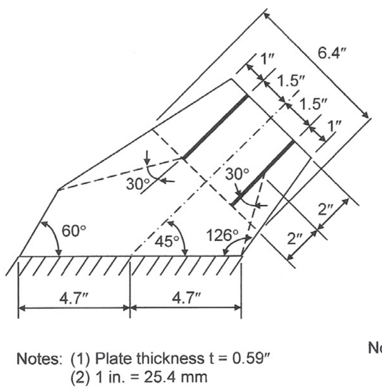

(a) Dimensions of gusset plate

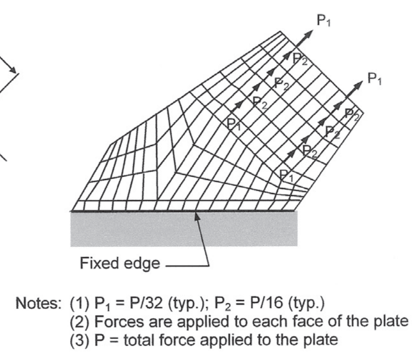

(b) Computer model and applied forces

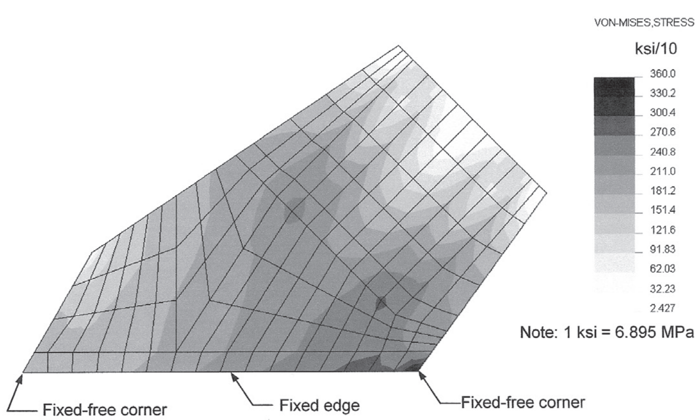

(c) Von Mises stress distribution at P = 85.3 kips (379 KN)

Fig. 13. Gusset plate model B2 for a 45° bracing-member-to- main-member connection.

starts at the end of the welded joint [where the von Mises stress reaches 36 ksi (248 MPa)] when the total applied tensile force, *P*, reaches 107.0 kips (476 kN), as shown in Figure 14(c).

OPTIMAL GUSSET PLATE CONFIGURATIONS

Based on the von Mises stress distributions on the plates shown in Figures 9(c) through 14(c), one can conclude that there are two possible places at which the stress concentration may occur. They are (1) the end of the welded joint [Figures 9(c), 10(c) and 14(c)] and (2) the fixed-free corner(s) [Figures 11(c), 12(c) and 13(c)] of the plate. Also, based on the tensile yielding capacities of the plates shown in Figures 9(c) through 14(c), one can conclude that the yielding capacity of a gusset plate will be reduced significantly if the stress concentration occurring at the fixed-free corner(s) of the plate caused by the stress singularity effect cannot be avoided or mitigated. In order to avoid and/or mitigate the stress concentration occurring at the fixed-free corners of the gusset plate due to the stress singularity effect, the optimal gusset plate configurations for bracing-member-to-main-member connections with various connection angles are recommended and are presented in Table 1.

As shown in cases (a) and (b) of Table 1, the base line (the line along the fixed edge) of each gusset plate is intersected by two 30° Whitmore lines. The base length (the fixed-edge length, *L*) of the gusset plate is the distance between the two intersections. Note that each 30° Whitmore line starts from one side of the weld lines. The locations of the starting points of the 30° Whitmore lines are determined by the degree of the angle θ, which is formed by the centerline of the bracing member and the centerline of the main member.

For cases (c) and (d) of Table 1, the base line of each gusset plate is equally divided by the centerline of the bracing member. One end of the base line is intersected by one of the 30° Whitmore lines at the obtuse angle of the gusset plate while the other end of the base line is terminated by a 60°

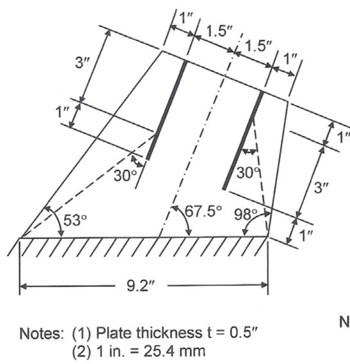

(a) Dimensions of gusset plate

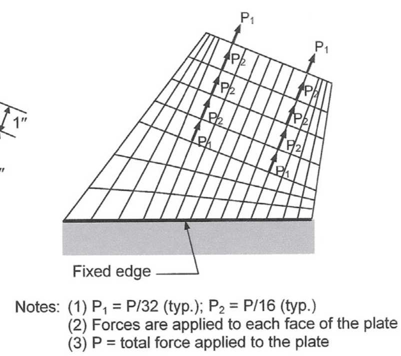

(b) Computer model and applied forces

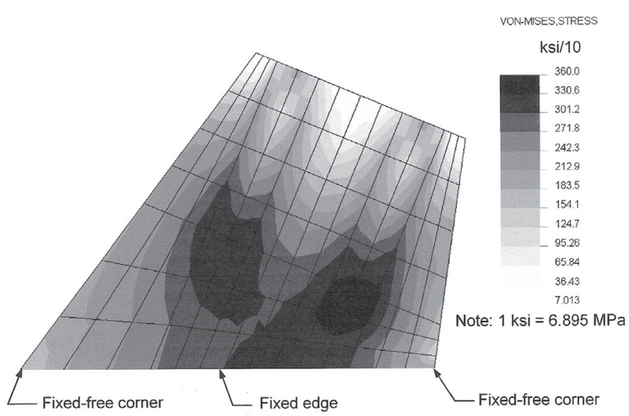

(c) Von Mises stress distribution at P = 107.0 kips (476 KN)

Fig. 14. Gusset plate model C1 for a 67.5° bracing-member-to- main-member connection.

Table 1. Optimal Gusset Plate Configurations for Bracing-Member-to-Main-Member Connections

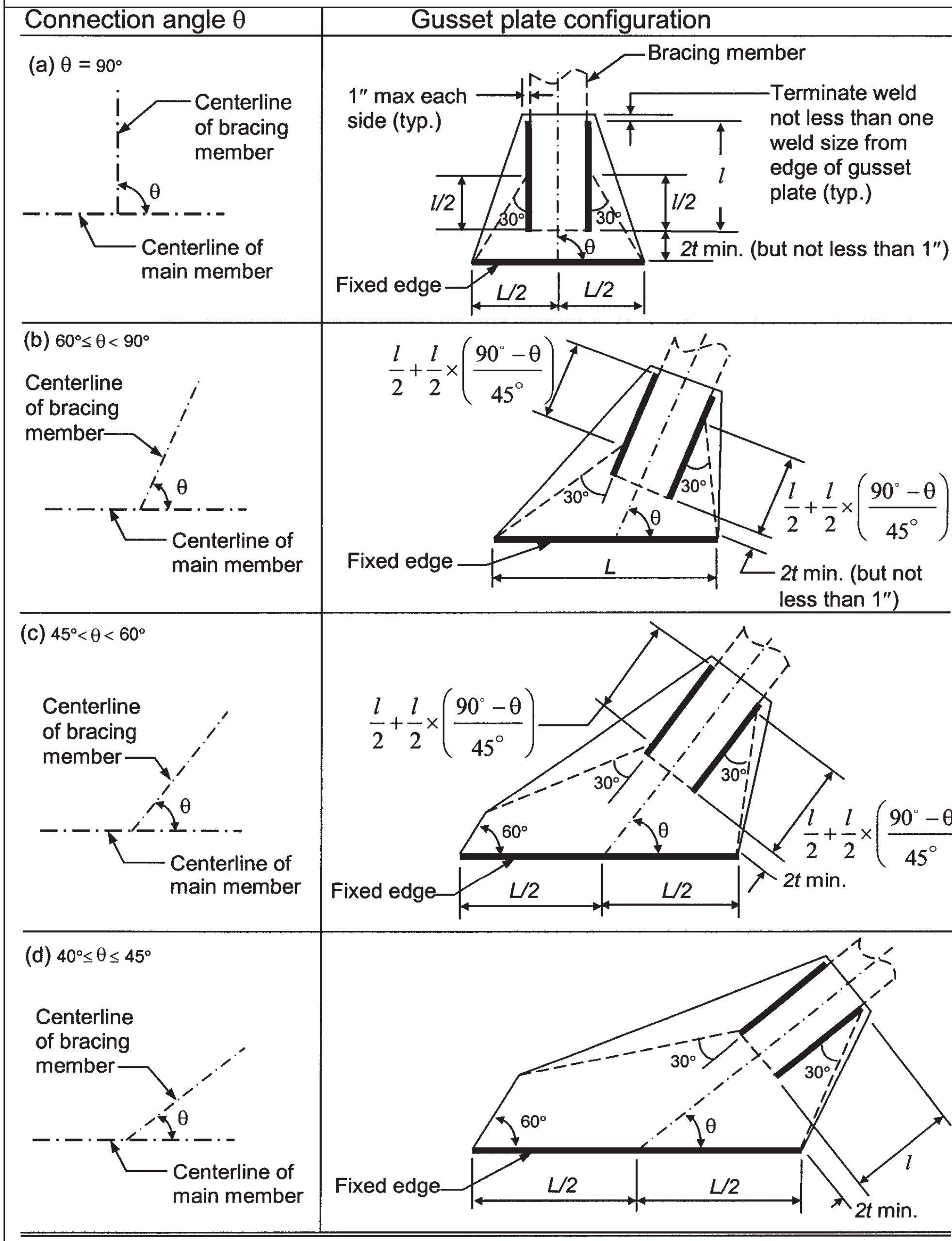

Notes: L = length of fixed edge
l = length of weld
t = thickness of gusset plate

inclined free edge. Furthermore, the top of the 60° free edge is intersected by the other 30° Whitmore line. Also, each 30° Whitmore line starts from one side of the weld lines. The locations of the starting points of the 30° Whitmore lines are determined by the degree of the angle θ, which is formed by the centerline of the bracing member and the centerline of the main member.

Note that a minimum length of "two times the gusset plate thickness" [but not less than 1 in. for cases (a) and (b)] between the end of the bracing member and the welded base line of the gusset plate is provided for each gusset plate. The purpose of the provided distance is to keep the welded base connection (the connection between the gusset plate and the main member) away from the stress concentration occurring at the end of the welded bracing-element-to-gusset-plate connection.

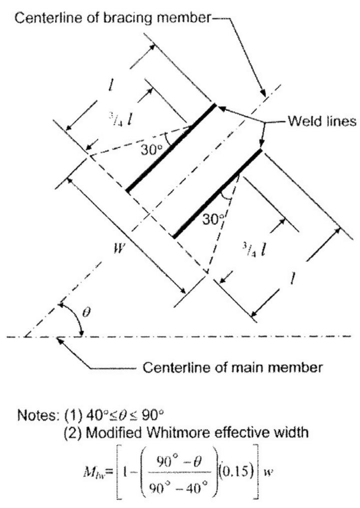

Fig. 15. Modification of Whitmore effective width for gusset plate in tension.

MODIFICATION OF WHITMORE EFFECTIVE WIDTH FOR GUSSET PLATE IN TENSION

Based on the outcomes of the analysis of numerous finite element models with various locations of Whitmore lines, an equation for the computation of the modified Whitmore effective width, M_{lw}, is introduced and is shown in Figure 15. The modified Whitmore effective width can be used to compute the tensile yielding capacity of a gusset plate for a 40° to 90° bracing-member-to-main-member connection. The following examples validate the accuracy of the modified Whitmore effective widths.

Example 1. Gusset plate model A1 for a 90° bracing-member-to-main-member connection: Referring to Figures 9(a) and 15, the modified Whitmore effective width, M_{lw}, shown in Figure 15 for the gusset plate A1 is 6.46 in. (164 mm). Note that the weld length, l, shown in Figure 15 for the gusset plate model A1 is 4 in. (102 mm). Using $P_y = A_e\, F_y$, one has P_y = (6.46 in. × 0.375 in.) × 36 ksi = 87.2 kips (388 kN).

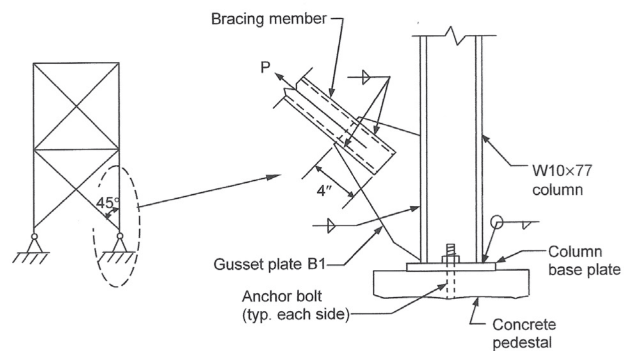

(a) Connection details

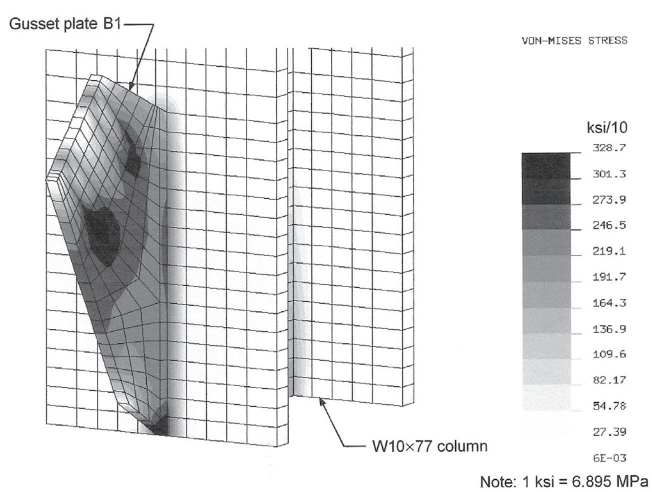

(b) Von Mises stress distribution at P = 100.8 kips (448 KN) applied to gusset plate B1

Fig. 16. Gusset plate to column connection (gusset plate in the same plane as column web) (Figure 16(a) shows an as-built detail that predates the OSHA requirement that a minimum of four anchor rods be used in a base plate).

Table 2. Summary of Nominal Tensile Yield Strengths Computed by Using the Modified-Whitmore-Effective-Width and Finite-Element Methods		
Guset plate	Nominal tensile yield strength computed by using the modified-Whitmore-effective-width mehtod	Nominal tensile yield strength computed by using the finite-element method
A1	87.2 kips (388 KN)	88.1 kips (392 KN)
A2	102.3 kips (455 KN)	101.9 kips (453 KN)
B1	100.6 kips (447 KN)	100.8 kips (448 KN)
C1	108.5 kips (483 KN)	107.0 kips (476 KN)

Note that P_y is the nominal tensile yield strength of the gusset plate, A_e is the modified Whitmore effective section of the gusset plate under tension, and F_y is the specified minimum yield stress of A36 steel. Also note that the computed tensile yielding capacity of the gusset plate A1 is 88.1 kips (392 kN) using the finite element method as shown in Figure 9(c).

Example 2. Gusset plate model A2 for a 90° bracing-member-to-main-member connection: Referring to Figures 10(a) and 15, the modified Whitmore effective width, M_{lw}, shown in Figure 15 for the gusset plate A2 is 6.46 in. (164 mm). [Note that the weld length, *l*, shown in Figure 15 for the gusset plate model A2 is 4 in. (102 mm)]. Therefore, the nominal tensile yield strength of the gusset plate, $P_y = A_e F_y$ = (6.46 in. × 0.44 in.) × 36 ksi = 102.3 kips (455 kN). Note that the computed tensile yielding capacity of the gusset plate A2 is 101.9 kips (453 kN) using the finite element method as shown in Figure 10(c).

Example 3. Gusset plate model B1 for a 45° bracing-member-to-main-member connection: Referring to Figures 12(a) and 15, the modified Whitmore effective width, M_{lw}, shown in Figure 15 for the gusset plate B1 is 5.59 in. (142 mm). [Note that the weld length, *l*, shown in Figure 15 for the gusset plate model B1 is 4 in. (102 mm)]. Therefore, the nominal tensile yield strength of the gusset plate, $P_y = A_e F_y$ = (5.59 in. × 0.5 in.) × 36 ksi = 100.6 kips (447 kN). Note that the computed tensile yielding capacity of the gusset plate B1 is 100.8 kips (448 kN) using the finite element method as shown in Figure 12(c).

Example 4. Gusset plate model C1 for a 67.5° bracing-member-to-main-member connection: Referring to Figures 14(a) and 15, the modified Whitmore effective width, M_{lw}, shown in Figure 15 for the gusset plate C1 is 6.03 in. (153 mm). [Note that the weld length, *l*, shown in Figure 15 for the gusset plate model C1 is 4 in. (102 mm)]. Therefore, the nominal tensile yield strength of the gusset plate, $P_y = A_e F_y$ = (6.03 in. × 0.5 in.) × 36 ksi = 108.5 kips (483 kN). Note that the computed tensile yielding capacity of the gusset plate C1 is 107.0 kips (476 kN) using the finite element method as shown in Figure 14(c).

A summary of the nominal tensile yield strengths of the gusset plates computed by using the modified-Whitmore-effective-width method and the finite-element method is shown in Table 2. Note that the modified-Whitmore-effective-width method shall only be applied to these gusset plates with optimal configurations as shown in Table 1 or to any other gusset plates without the stress singularity effect. The modified-Whitmore-effective-width method should not be applied to the gusset plates A3 (Figure 11) and B2 (Figure 13) since their tensile yielding capacities are significantly controlled by the stress singularity effect at their fixed-free corners. If the fixed-free corners of a gusset plate are larger than that shown in Table 1, the strength of the gusset plate is expected to be significantly controlled by the stress singularity effect at its fixed-free corners. In this case, a finite element model is needed for the determination of the strength of the fixed-free corners of the gusset plate.

EXAMPLES OF GUSSET PLATES FRAMED TO SUPPORT MEMBERS

In order to validate the fixed-edge boundary condition of the gusset plate B1 shown in Figure 12, two examples of the gusset-plate-to-support-member connections are illustrated as the following.

The example of the gusset-plate-to-column connection shown in Figure 16(a) indicates (1) the gusset plate is in the same plane as the column web, and (2) the angle between the bracing member and the column is 45°. A finite element model has been constructed to simulate this connection. The gusset plate size used in the model is B1, which is the same size as that shown in Figure 12. The column size and length are W10×77 and 12 ft, respectively, in this model. Also, the column has been modeled to be fixed at its top and bottom ends. The same tensile force [P = 100.8 kips (448 kN)] that has been applied to the gusset plate B1 shown in Figure 12 is also applied to the gusset plate in this model.

Figure 16(b) shows the result of the finite element analysis for this model. The result indicates that the maximum von Mises stress occurring in the gusset plate is only 328.7 ksi/10 or 32.9 ksi (227 MPa), which is lower than the maximum von Mises stress [360.0 ksi/10 or 36.0 ksi (248 MPa)] shown in Figure 12(c). The result also indicates that the yielding capacity of the gusset plate computed in this example is about 9 percent [= (36.0 ksi / 32.9 ksi) – 1] higher than that of the same gusset plate computed in Figure 12(c). This example demonstrates that the simplified fixed-edge boundary condition of the gusset plate B1 shown in Figure 12 is acceptable for the computation of the yielding capacity of the gusset plate connected to a column as shown in Figure 16.

The example of the gusset-plate-to-column connection shown in Figure 17(a) indicates (1) the gusset plate is perpendicular to the plane of the column web, (2) half-inch horizontal and vertical stiffeners (note that the vertical stiffener is in the same plane as the gusset plate) are welded to the far side of the column web in order to provide a relatively rigid support for the gusset plate, and (3) the angle between the bracing member and the column is 45°. A finite element model has been constructed to simulate this connection. The gusset plate size used in the model is B1, which is the same size as that shown in Figure 12. The column size and length are W10×77 and 12 ft, respectively, in this model. Also, the column has been modeled to be fixed at its top and bottom ends. The same tensile force [P = 100.8 kips (448 kN)] that has been applied to the gusset plate B1 shown in Figure 12 is also applied to the gusset plate in this model.

Figure 17(b) shows the result of the finite element analysis for this model. The result indicates that the maximum von

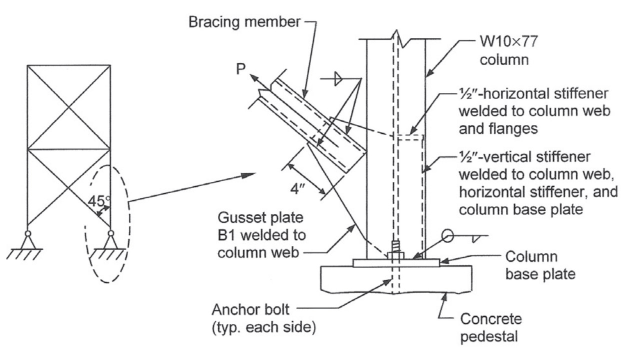

(a) Connection details

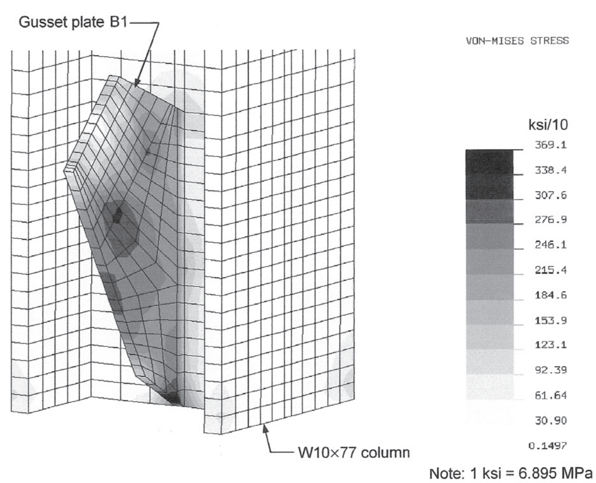

(b) Von Mises stress distribution at P = 100.8 kips (448 KN) applied to gusset plate B1

Fig. 17. Gusset plate to column connection (gusset plate perpendicular to the plane of column web) (Figure 17(a) shows an as-built detail that predates the OSHA requirement that a minimum of four anchor rods be used in a base plate).

Mises stress occurring in the gusset plate is 369.1 ksi/10 or 36.9 ksi (254 MPa) which is slightly higher than the maximum von Mises stress [36.0 ksi (248 MPa)] shown in Figure 12(c). The result also indicates that the yielding capacity of the gusset plate in this example is slightly lower (within 3 percent) than that of the same gusset plate in Figure 12(c). This example therefore also validates the fixed-edge boundary condition of the gusset plate B1 shown in Figure 12.

DESIGN EXAMPLE

The following example illustrates the application of the recommended optimal configuration and modified Whitmore effective width for the design of a gusset plate in a steel truss.

Design Example:

Design a gusset plate for a 90° bracing-member-to-main-member connection in an earthquake-resistant steel truss. Assume that (1) two angles, L3×3×⅜, are to be used as the bracing member, (2) ASTM A36 steel is to be used for both the bracing member and the gusset plate, and (3) E70XX electrodes having a minimum tensile strength of 70 ksi (483 MPa) are to be used for the fillet weld made by shielded metal arc welding (SMAW).

Solution:

1. Compute axial tension yield capacity of the bracing member. In order to avoid brittle failure of connections, the capacity of the welded connection is recommended to be at least equal to or greater than the axial tension yield capacity of the bracing member computed using a conservative expected yield stress of $1.1R_yF_y$ (Astaneh-Asl, 1998). Note that R_y = ratio of the expected yield strength to the specified minimum yield strength of the grade of steel to be used (AISC, 2002). For ASTM A36 steel angles, $R_y = 1.5$. Therefore, the axial tension yield capacity of the bracing member (2L3×3×⅜) = $1.1R_yF_yA_g$ = 1.1(1.5)(36 ksi)(4.22 in.^{2}) = 250.7 kips (1115 kN). Note that A_g = cross-sectional area of 2L3×3×⅜. Thus, the axial tension yield capacity of each angle = 125.3 kips (558 kN).

2. Determine the lengths of fillet weld to be used for the bracing member-to-gusset plate connection (AISC, 2001). Assuming the gusset plate thickness = ¾ in. (19 mm), the minimum size of fillet weld shall be not less than ¼ in. (6.4 mm). Also, since the thickness of the bracing member is ⅜ in., the maximum size of the fillet weld shall be 5⁄16 in. (7.9 mm) (= ⅜ in. – 1⁄16 in.). Using a 5⁄16 in. fillet weld, calculate the weld strength as follows.

   Effective throat, t_e = (5⁄16 in.)(0.707) = 0.221 in. (5.6 mm)

$$\begin{aligned}\text{Capacity of weld per inch} &= 0.75t_e(0.60F_{EXX}) \\ &= 0.75(0.221\text{ in.})(0.60)(70\text{ ksi}) \\ &= 6.96\text{ kips/in. } (1.22\text{ kN/mm})\end{aligned}$$

where F_{EXX} is the electrode classification number (specified minimum strength).

Referring to Figure 18, the strength of weld at the end of the angle is

$$\phi\left(0.6F_{EXX}\right)\left(1.0+0.50\sin^{1.5}\theta\right)A_w$$
$$= 0.75\left(0.6\times 70\text{ ksi}\right)\left(1.0+0.50\sin^{1.5}90°\right)\left(0.221\text{ in.}\right)\left(3\text{ in.}\right)$$
$$= 31.3\text{ kips}\left(139\text{ kN}\right)$$

where A_w is the effective area of the weld throat.

Thus, F_2 = 31.3 kips (139 kN).

From the moment equilibrium about the left bottom point of the angle,

$$F_1 = \frac{\left(125.3\text{ kips}\right)\left(2.116\text{ in.}\right)-\left(31.3\text{ kips}\right)\left(1.5\text{ in.}\right)}{3\text{ in.}}$$
$$= 72.7\text{ kips}\left(324\text{ kN}\right)$$

From the vertical force equilibrium,

F_3 = 125.3 – 72.7 –31.3 = 21.3 kips (95 kN)

Thus, the length of the weld along the back of the angle is

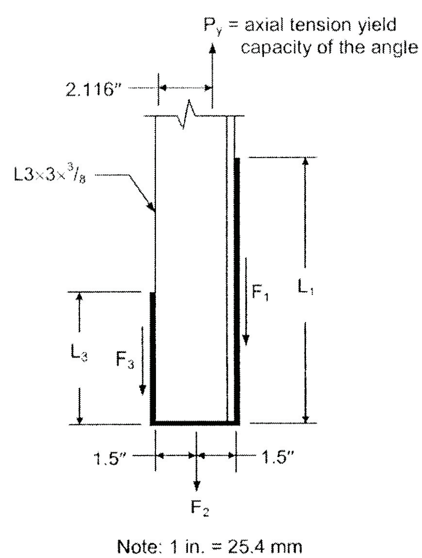

Fig. 18. Forces acting at angle to gusset plate connection.

$$L_1 = \frac{72.7 \text{ kips}}{6.96 \text{ kips/in.}} = 10.40 \text{ in.}$$

Use $L_1 = 10$ in. (254 mm)

The length of the weld along the toe of the angle is

$$L_3 = \frac{21.3 \text{ kips}}{6.96 \text{ kips/in.}} = 3.06 \text{ in.}$$

Conservatively use $L_3 = 5$ in. (127 mm)

Note that the balanced welds (the center of gravity of the weld group coincides with the center of gravity of the member) are desirable; however, the balanced welds are not required for statically-loaded single angle, double angle, and similar members (AISC, 2001).

3. Determine the thickness of the gusset plate using the modified Whitmore effective section. In order to achieve a ductile behavior, yielding of the bracing member shall be designed to occur first, followed by yielding of the gusset plate (Astaneh-Asl, 1998). Based on this design concept, the following equation is suggested for the determination of the gusset plate thickness (note that the modified Whitmore effective area, A_e, is suggested to be used here to compute the yield capacity of the gusset plate):

$$R_y F_y A_g \leq F_y A_e \tag{1}$$

where

R_y = 1.5 for ASTM A36 steel angles (bracing member)
F_y = 36 ksi for ASTM A36 steel
A_g = cross area of double angles (bracing member)
A_e = the area of the modified Whitmore effective section for the gusset plate

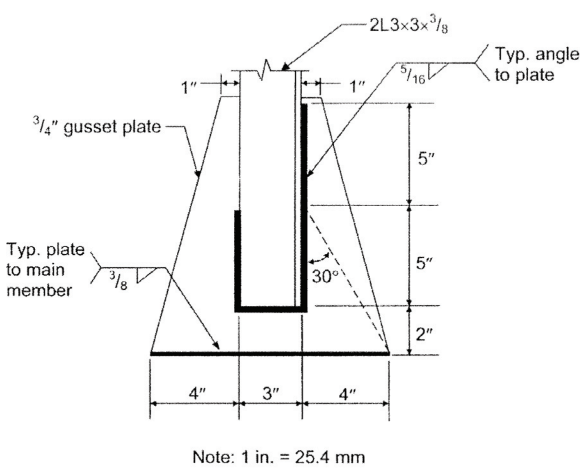

Fig. 19. Details of gusset plate.

Referring to Figure 15, the modified Whitmore effective width for the plate,

$$M_{lw} = (¾)(10 \text{ in.})(\tan 30°) + 3 \text{ in.} + (¾)(5 \text{ in.})(\tan 30°)$$
$$= 9.50 \text{ in. (241 mm)}$$

Therefore, the area of the modified Whitmore effective section, $A_e = 9.50t$ in.[2] Note that t is the thickness of the gusset plate.

From Equation 1,

$$1.5(36)(4.22) \leq 36(9.50t)$$

Therefore, the minimum required $t = 0.67$ in. (17 mm).

Use plate thickness $t = ¾$ in. (19 mm).

4. Determine the configuration of the gusset plate. Based on case (a) of Table 1, the configuration of the gusset plate is determined and is shown in Figure 19. Note that the configuration of the right side of the gusset plate shown in Figure 19 follows the configuration that is shown in case (a) of Table 1. The configuration of the right side of the gusset plate is then mirrored and reproduced on the left side of the gusset plate for symmetry. Also note that the distance between the end of the bracing member and the base line of the gusset plate shown in Figure 19 is 2 in. (51 mm). The distance provided is slightly larger than the recommended distance $2t$ [= 2 × ¾ in. = 1.5 in. (38 mm)] in order to accommodate the ⁵⁄₁₆ in. (7.9 mm) of the welding along the end of the bracing element as well as the size of the welding along the face of the main element. Assume that a ⅜ in. fillet weld is required along the base line and on each face of the gusset plate as shown in Figure 19. Based on Figure 19, the actual effective width provided by the gusset plate is shown in Figure 20. Since the actual effective width for tension is only 8.67 in. (220 mm), which is less than the modified Whitmore effective width [= 9.5 in. (241 mm)], the minimum required thickness for the gusset plate is recomputed by using Equation 1:

$$1.5(36)(4.22) \leq 36(8.67t)$$

From which, the minimum required $t = 0.73$ in. (19 mm). Since the thickness required (0.73 in.) is less than the thickness actually provided (0.75 in.), the thickness provided for the gusset plate satisfies Equation 1.

5. Check fracturing of the net area of the gusset plate using the modified Whitmore effective section. In order to ensure the ductility of the gusset plate, fracturing of the net area of the gusset plate should not occur prior to yielding of the gusset plate (Astaneh-Asl, 1998). Based

on this design criterion, the following equation is suggested to be used to check the net area fracturing of the gusset plate (note that the modified Whitmore effective section is suggested to be used here to compute both the net area fracture capacity, as well as the yield capacity of the gusset plate):

$$0.75A_{ne}F_u \geq 0.9\ (1.1R_yA_eF_y) \quad (2)$$

where

A_{ne} = the net area of the modified Whitmore effective section of the gusset plate
F_u = 58 ksi for ASTM A36 steel
R_y = 1.1 for steel plates (AISC, 2002)
A_e = the area of the modified Whitmore effective section of the gusset plate
F_y = 36 ksi for ASTM A36 steel

Note that the actual effective width of the gusset plate has been found to be 8.67 in. (220 mm). Therefore,

$$A_e = 8.67\ (3/4) = 6.50 \text{ in.}^2\ (4190 \text{ mm}^2)$$

Also, since $A_{ne} = A_e$ for a welded connection (there are no bolt holes in the gusset plate), one has $0.75A_{ne}F_u$ = 0.75(6.50)(58) = 283 kips (1260 KN), and $0.9\ (1.1R_yA_eF_y)$ = 0.9(1.1)(1.1)(6.50)(36) = 255 kips (1130 kN)

The computation shown above indicates that Equation 2 is satisfied. Therefore, fracturing of the net area of the gusset plate will not occur prior to yielding of the gusset plate.

6. Check for block shear rupture of the gusset plate. Block shear rupture of the gusset plate shall also be checked to ensure that the block shear capacity of the gusset plate is greater than the yield capacity of the gusset plate. However, since the bracing-member-to-gusset-plate connection shown in Figure 19 has relatively long paths to resist shear forces [the total length of the shear paths is 20 in. (508 mm) long], by inspection one can conclude that the block shear failure mode of the gusset plate will not govern the yield failure mode of the gusset plate.

7. Check the von Mises and first principal stresses distributions along the gusset plate using the finite element method. Based on the details of the welded brace member gusset plate assembly shown in Figure 19, a finite element model was constructed in order to investigate its von Mises stress distribution at first yield as well as its first principal stress distribution at ultimate condition. Nonlinear static analysis was conducted for the model using the computer software Nisa II / Display III. ASTM A36 steel was used for both the gusset plate and the bracing member. The elastic, piecewise linear hardening stress-strain curve shown in Figure 6 was used as the material property for the A36 steel. The E7018 electrode was used for the fillet weld. The elastic, linear hardening stress-strain curve shown in Figure 7 was used as the material property of the E7018 electrode for the fillet weld. The results of the analysis for the assembly subjected to tensile forces are shown in Figures 21 and 22.

   Note that in order to consider the effect of strain hardening of the A36 steel as shown in Figure 6, an arbitrary tensile stress of 60 ksi (414 MPa) was applied at the free end of the double angles. A pseudo time of 10.0 was used

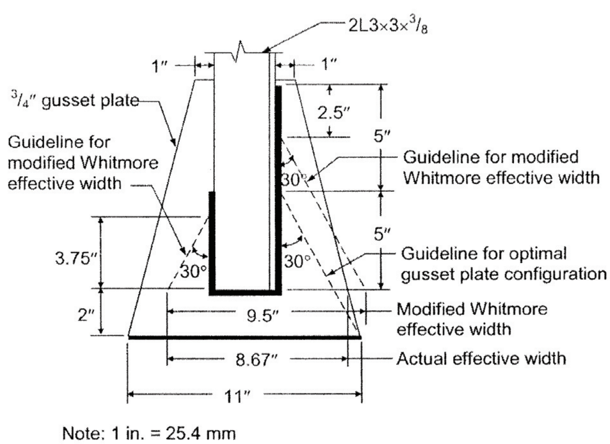

Fig. 20. Actual effective width of the gusset plate under tension.

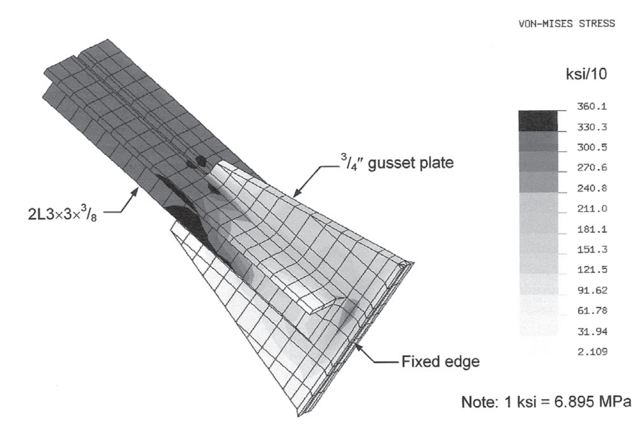

Fig. 21. Von Mises stress distribution at first yield of the brace member—gusset plate assembly.

for the time span that is equivalent to load increments or steps [from zero to 60 ksi (414 MPa)]. When the time step reached 5.4 as shown in Figure 21, the applied stress at the free end of the double angle reached 32.4 ksi (223 MPa) [= 60 ksi × (5.4/10)]. At this time step, the von Mises stress (related to yielding) exceeded 36 ksi (248 MPa) in some areas within the bracing member rather than the gusset plate. This result satisfies the design criterion mentioned in step 3 of this design example.

Also, when the time step reached 6.6 as shown in Figure 22, the applied stress at the free end of the double angle reached 39.6 ksi (273 MPa) [= 60 ksi × (6.6/10)]. At this time step, the first principal stress (related to fracturing) exceeded 58 ksi (400 MPa) (= F_u, the specified tensile strength of the A36 steel) in the area within the bracing member (close to the free end of the gusset plate as shown in Figure 22) rather than in the gusset plate. This result indicates that when the bracing member is under great tension, fracturing is expected to occur at the cross section of the double angles near the free end of the gusset plate. Also note that when the first principal stress exceeded F_u in the bracing member, the maximum first principal stress distribution within the gusset plate (near the ends of the double angles as shown in Figure 22) is only 40.1 ksi (277 MPa). Therefore, fracturing in the gusset plate will not occur.

CONCLUSIONS

Stress singularity (unbounded stress) effect caused by the boundary condition at the corners of the fixed edges of welded gusset plates was pointed out in this paper. Numerical investigations were carried out to study the interaction between the stress singularity effect and the Whitmore effective width for welded gusset plates under tension. The results of the investigations are summarized as follows:

1. If yielding is expected to start at the critical cross section (in other words, at the end of the welded joint) of a gusset plate, the tensile yielding capacity of the gusset plate can be increased more effectively by increasing the thickness of the plate rather than the width of the plate.

2. If yielding is expected to start at the fixed-free corners of a gusset plate, the tensile yielding capacity of the gusset plate can be increased more effectively by increasing the width at the base of the plate rather than the thickness of the plate. Increasing the width at the base of the plate will reduce the angle at the fixed-free corners, which in turn will mitigate the stress singularity effect on these corners.

Based on these conclusions, optimal configurations as well as modifications of the Whitmore effective width for the design of gusset plates loaded in tension were proposed. Later in this paper a practical design demonstration which incorporated both the optimal configuration and the modified Whitmore effective section for the design of a gusset plate was given. The finite element method, which incorporates the effect of material nonlinearity, was then used to validate the expectation that the fracture strength of the gusset plate is larger than that of the bracing element.

It should be realized that the results presented in this paper are based on finite element analysis alone. Physical testing in the lab is required to verify the results, and before implementation of the proposed procedure.

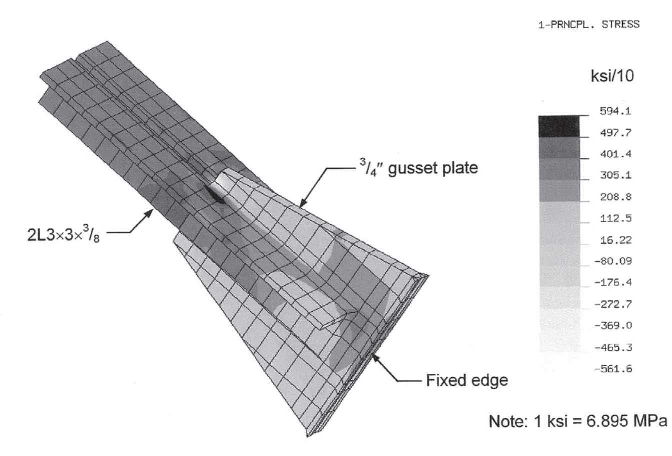

Fig. 22. First-principal stress distribution at ultimate condition of the brace member—gusset plate assembly.

ACKNOWLEDGMENTS

Funding for this research was provided by the Office of Research Development and Administration, the College of Engineering, and the Department of Civil and Environmental Engineering at the Southern Illinois University at Carbondale. Their support is gratefully acknowledged.

REFERENCES

AISC (2001), *Load and Resistance Factor Design Manual of Steel Construction*,3rd Edition, American Institute of Steel Construction, Inc., Chicago, IL.

AISC (2002), *Seismic Provisions for Structural Steel Buildings*, May 21, 2002, American Institute of Steel Construction, Inc., Chicago, IL.

Astaneh-Asl, A. (1989), "Simple Methods for Design of Steel Gusset Plates," *ASCE Steel Structures*, May 1-5, pp. 345-354.

Astaneh-Asl, A. (1998), “Seismic Behavior and Design of Gusset Plates,” Steel Tips Report, Structural Steel Educational Council, Moraga, CA.

Astaneh-Asl, A., Goel, S.C., and Hanson, R.D. (1982), “Cyclic Behavior of Double Angle Bracing Members with End Gusset Plates,” Report No. UMEE 82R7, University of Michigan, Ann Arbor, MI.

Bjorhovde, R. (1988), “Limit States Design Considerations for Gusset Plates,” *Journal of Constructional Steel Research*, Vol. 9, No. 1, pp. 61-73.

Bjorhovde, R., and Chakrabarti, S.K. (1985), “Tests of Full-Size Gusset Plate Connections,” *Journal of Structural Engineering*, ASCE, Vol. 111, No. 3, March, pp. 667-684.

Cheng, J.J.R., Grondin, G.Y., and Yam, M.C.H. (2000), “Design and Behavior of Gusset Plate Connections,” Steel Connection IV Workshop, Roanoke, VA.

Gross, J.L. (1990), “Experimental Study of Gusseted Connections,” *Engineering Journal*, AISC, Vol. 27, No. 3, 3rd Quarter, pp. 89-97.

Hardash, S.G., and Bjorhovde, R. (1985), “New Design Criteria for Gusset Plates in Tension,” *Engineering Journal*, AISC, Vol. 22, No. 2, 2nd Quarter, pp. 77-94.

Hsiao, J.K. (2000), *Strength and Ductility of the Enlarged Beam Section Connection: A New Fully-Restrained Steel Moment Connection*, Ph.D. Thesis, Department of Civil and Environmental Engineering, University of Utah, UMI Dissertation Services, Ann Arbor, MI.

NISA (1998), *NISA User's Manual*, Engineering Mechanics Research Corporation, Troy, MI.

Salmon, C.G., and Johnson, J.E. (1996), S*teel Structures, Design and Behavior*, 4th Edition, Prentice-Hall, Inc., Upper Saddle River, NJ.

The Lincoln Electric Company (1994), *The Procedure Handbook of Arc Welding,* 13th Edition, The Lincoln Electric Company, Cleveland, OH.

Whitmore, R.E. (1952), “Experimental Investigation of Stresses in Gusset Plates,” Bulletin No. 16, Engineering Experiment Station, University of Tennessee, TN.

Williams, M.L. (1952), “Stress Singularities Resulting from Various Boundary Conditions in Angular Corners of Plates in Extension,” *Journal of Applied Mechanics,* Vol. 19, No. 4, pp. 526-528.